Cell Motility and the Cytoskeleton 40:304–314 (1998)

In Vitro Microtubule-Based Organelle Transport in Wild-Type *Dictyostelium* and Cells Overexpressing a Truncated Dynein Heavy Chain

Nira Pollock,[1] Michael P. Koonce,[3] Eugenio L. de Hostos, [4] and Ronald D. Vale[1,2]*

[1]*Department of Pharmacology, University of California San Francisco, San Francisco, California*
[2]*Howard Hughes Medical Institute, University of California San Francisco, San Francisco, California*
[3]*Division of Molecular Medicine, Wadsworth Center, Empire State Plaza, Albany, New York*
[4]*Department of Biochemistry and Cell Biology, Rice University, Houston, Texas*

The transport of vesicular organelles along microtubules has been well documented in a variety of systems, but the molecular mechanisms underlying this process are not well understood. We have developed a method for preparing extracts from *Dictyostelium discoideum* which supports high levels of bidirectional, microtubule-based vesicle transport in vitro. This organelle transport assay was also adapted to observe specifically the motility of vesicles in the endocytic pathway. Vesicle transport can be reconstituted by recombining a high-speed supernatant with KI-washed organelles, which do not move in the absence of supernatant. Furthermore, a microtubule affinity-purified motor fraction supports robust bidirectional movement of the salt-washed organelles. The plus and minus end-directed transport activities can be separated by exploiting differences in their affinities for microtubules in the presence of 0.3 M KCl. We also used our assay to examine organelle transport in a strain of *Dictyostelium* overexpressing a 380-kDa C-terminal fragment of the cytoplasmic dynein heavy chain, which displays an altered microtubule pattern (380-kDa cells; [Koonce and Samso, Mol. Biol. Cell 7:935–948, 1996]). We have found that the frequency and velocity of minus end-directed membrane organelle movements were significantly reduced in 380-kDa cells relative to wild-type cells, while the frequency and velocity of plus end-directed movements were equivalent in the two cell types. The 380-kDa C-terminal fragment cosedimented with membrane organelles, although its affinity was significantly lower than that of native dynein. An impaired membrane-microtubule interaction may be responsible for the altered microtubule patterns in the 380-kDa cells. Cell Motil. Cytoskeleton 40:304–314, 1998.

Key words: vesicle transport; intracellular motility; microtubule-based motors

INTRODUCTION

The directed transport of vesicular organelles is an important component of intracellular sorting in eukaryotic cells. Cytoplasmic motor-driven movement of membrane organelles along microtubule or microfilament ''tracks'' has been documented in a wide variety of systems. In recent years, much progress has been made in

Contract grant sponsor: National Institutes of Health; Contract grant number: GM51532; Contract grant number: 38499; Contract grant sponsor: American Heart Association.

*Correspondence to: R.D. Vale, Department of Pharmacology, 513 Parnassus Ave., University of California San Francisco, San Francisco, CA 94143; E-mail: vale@phy.ucsf.edu

Received 13 February 1998; accepted 26 March 1998

assigning roles to motor proteins for specific cellular transport activities [Allan, 1995; Goodson et al., 1997]. However, the actual mechanisms by which motors bind to organelles and facilitate their movement are still largely a mystery.

To advance our understanding of microtubule-based organelle transport, it would be useful to study this process in a simple unicellular organism that offers the opportunity to combine biochemistry and genetics. Although the yeast *Saccharomyces cerevisiae* would appear to provide an attractive candidate for such a system, vesicle transport in this organism appears to be actin-based [Hill et al., 1996; Huffaker et al., 1988; Novick and Botstein, 1985]. In contrast, the cellular slime mold *Dictyostelium discoideum* has a radial array of microtubules emanating from a central microtubule organizing center or nucleus-associated body [Roos et al., 1984]; vesicles have been observed moving linearly along these microtubules, and motility was blocked by the microtubule depolymerizing drug nocodazole [Roos et al., 1987]. Intracellular vesicle sorting pathways in *Dictyostelium*, including endocytosis, phagocytosis, and secretion, have been well studied and appear similar to higher eukaryotes [Bacon et al., 1994; Lenhard et al., 1992; Ruscetti et al., 1994; Spudich, 1987]. *Dictyostelium* also has several experimental advantages, in that abundant starting material can be obtained for biochemical purifications and functions of particular genes can be tested by targeted disruption [De Lozanne and Spudich, 1987; Jung and Hammer, 1990; Kuspa and Loomis, 1994].

Studies of cytoplasmic microtubule-based motors in *Dictyostelium* have resulted in the purification of a 105-kDa kinesin-like protein [McCaffrey and Vale, 1989] and a cytoplasmic dynein [Koonce and McIntosh, 1990]. Like the dyneins of higher eukaryotes, *Dictyostelium* dynein is a complex composed of a 540-kDa heavy chain (DHC), an 85-kDa intermediate chain (IC), and at least two light chains (LC) of approximately 58 and 53 kDa [Koonce et al., 1994]. Because disruption of the DHC gene is lethal [Koonce and Knecht, 1998], Koonce and Samso [1996] constructed a series of *Dictyostelium* cell lines overexpressing various fragments of the dynein heavy chain (DHC) in order to define the function of cytoplasmic dynein in vivo. Unexpectedly, overexpression of a 380-kDa C-terminal heavy chain fragment encoding the dynein globular head (380-kDa cells; [Koonce and Samso, 1996]) generated a phenotype in which the interphase microtubule array lost its radial character and appeared collapsed toward the cell center. Koonce and Samso speculated that this phenotype could indicate a role for dynein in maintaining the spatial pattern of the interphase microtubule network. Like the full-length DHC, the 380-kDa fragment cosediments with microtubules in an ATP-dependent fashion and undergoes a UV-vanadate cleavage reaction. However, unlike the native DHC, it is unable to dimerize and does not bind either the 85-kDa IC or the 53-kDa LC, although it may weakly bind the 58-kDa LC. As these biochemical data alone do not explain the in vivo phenotype, additional functional studies are required. Clearly, an in vitro assay for organelle transport would be valuable for characterizing this and other microtubule-based motor mutants in *Dictyostelium*.

In this study, we report a method for preparing *Dictyostelium* extracts that support high levels of bidirectional microtubule-based vesicle motility in vitro and that can be used to study the motility of vesicles in the endocytic pathway. The velocities and qualitative aspects of these movements appear to replicate in vivo vesicle movements in *Dictyostelium* [Roos et al., 1987]. The combination of high-speed supernatants or fractions enriched in microtubule-based motor proteins with salt-washed vesicle fractions reconstitutes motility. Furthermore, factors involved in plus and minus end-directed motility can be separated based on differential microtubule affinity.

Our assay also has allowed us to take advantage of the first microtubule-based motor mutants created in *Dictyostelium* by examining the effects of the overexpression of the 380-kDa DHC fragment on organelle transport in vitro. We have found that the frequency and velocity of minus end-directed membrane organelle movements were specifically reduced in 380-kDa cells relative to wild-type cells, while the frequency and velocity of plus end-directed movements were equivalent in the two cell types. These results suggest that the in vivo phenotype of the 380-kDa cells may be linked to a defect in dynein-based organelle transport.

MATERIALS AND METHODS

Extract Preparation

Dictyostelium strain Ax-2 was grown in suspension at 22°C to a density of 4–8 $\times$ 10^6 cells/ml in HL-5 [Sussman, 1987] containing 100 μg/ml streptomycin and 100 U/ml penicillin. For the 380-kDa and 318-kDa cells, 10 μg/ml G418 (Geneticin; Gibco-BRL, Grand Island, NY) was also added. Approximately 6 $\times$ 10^8–1.2 $\times$ 10^9 cells were collected by centrifugation at 800*g* for 3 min in a clinical centrifuge at room temperature. The cell pellet was placed on ice, washed once with ice-cold Sorenson's phosphate buffer, pH 6.0 [Malchow et al., 1972], recentrifuged, and then resuspended in 1:1 w/v lysis buffer (LB: 30 mM Tris-HCl (pH 8), 4 mM EGTA, 3 mM DTT, 5 mM benzamidine, 10 μg/ml soybean trypsin inhibitor, 5 μg/ml TPCK/TAME, 10 μg/ml leupeptin, pepstatin A, and chymostatin, and 5 mM PMSF (phenylmethyl-sulfonyl fluoride) containing 30% (w/v) sucrose. Cells were lysed

by one passage through a Nuclepore polycarbonate filter (5-μm pore size, 25-mm diameter; Costar, Pleasanton, CA) using a 10-ml syringe. The lysate was centrifuged at 2,000*g* for 5 min at 4°C, and the resulting postnuclear supernatant (PNS) was layered over a 1-ml cushion of LB/25% sucrose and centrifuged in a Beckman TLA 100.4 rotor at 180,000*g* for 15 min at 4°C. The high-speed supernatant (HSS) was removed, and the vesicle pellet was resuspended in LB/15% sucrose (one-half volume of the original PNS). To prepare salt-washed vesicles, LB containing 1.2 M KI was added to the resuspended pellet to achieve a final concentration of 0.3 M KI. After incubation for 30 min on ice, membranes were diluted by adding 2 vol of LB/15% sucrose and centrifuged as before over a 1-ml cushion of LB/25% sucrose in a Beckman TLA 100.4 rotor. The cushion was aspirated, and the salt-washed membranes were resuspended in LB/30% sucrose (0.3 vol of the original PNS). 15-μl aliquots of the resuspended vesicles were frozen in liquid nitrogen and, upon thawing, 0.5 μl of fresh 1M PMSF was added.

Preparation of Extracts with Labeled Endocytic Vesicles

Approximately 8×10^8 cells were pelleted as described above and resuspended in 5 ml HL5 (final cell density 1.6×10^8 cells/ml) at room temperature (25°C). Cells were incubated for 10 min at 22°C while shaking at 180 rpm to recover endocytic function. To begin the pulse, 2.5 ml of HL5 containing 4 mg/ml rhodamine-conjugated dextran (tetramethyl rhodamine-conjugated dextran, 40,000 MW, neutral; Molecular Probes, Eugene OR) was added (final densities 1.1×10^8 cells/ml, 1.33 mg/ml dextran). Cells were incubated for 20 min while shaking at 180 rpm and then pelleted by centrifugation. Cells were washed twice with 50 ml Soerenson's phosphate buffer at 4°C and processed to a lysate as described above.

Preparation of ATP Releasate

Cells (1–3 l at a density of 4–8 $\times$ 10^6 cells/ml) were washed and lysed as described above, the only exception being that a 47-mm diameter filter and 30-ml syringe were used. A HSS was prepared as described above and incubated with 15 U/ml hexokinase, 3 mM glucose, 4 mM AMP-PNP/$MgCl_2$, and 20 μM taxol. Prior to preparation of the extract, bovine brain tubulin at approximately 2.5 mg/ml was polymerized with 10% DMSO and 1 mM GTP in 40 mM K-Pipes, pH 6.8, 0.5 mM EGTA, 2 mM $MgCl_2$ (0.5$\times$ BRB80) and 20 μM taxol by incubation for 10 min at 37°C. The microtubules were collected by centrifugation at 360,000*g* for 10 min in a Beckman TLA 120.1 rotor (22°C), and resuspended in the HSS (plus hexokinase, glucose, AMP-PNP, and taxol as above) for a final tubulin concentration of 0.5 mg/ml. The HSS/microtubule mix was incubated on ice for 20 min; microtubules and associated proteins were then centrifuged through a 1-ml cushion of LB/25% sucrose containing 20 μM taxol at 85,000*g* for 15 min in a Beckman TLA 100.4 rotor (4°C). The microtubule pellet was resuspended in LB/5% sucrose containing 5 mM ATP/$MgCl_2$ (1:20 vol of the original HSS volume) and incubated on ice for 15 min to release bound motor proteins. Microtubules were separated from the released proteins by centrifuging at 90,000*g* for 15 min in a Beckman TLA 120.1 rotor (4°C). The supernatant (ATP release) was collected and either frozen in liquid nitrogen or assayed directly (see below). To separate plus end- and minus end-directed transport activities, the microtubule pellet obtained after the initial incubation of microtubules with the HSS was resuspended in LB/5% sucrose containing 0.3 M KCl (1:20 vol of the original HSS volume) and immediately recentrifuged at 85,000*g* for 15 min in a Beckman TLA 100.4 rotor (4°C). The resulting supernatant (''salt wash'') was dialyzed for 70 min against LB/5% sucrose using a microdialyzer system 100 (Pierce, Rockford, IL), exchanging the buffer in the chamber once after 30 min of dialysis. In parallel, the microtubule pellet was resuspended in LB/5% sucrose containing 5 mM ATP/$MgCl_2$ to elute the remaining motors as described above.

Organelle Transport Assays

Preparation of axoneme-nucleated MT structures. Flow cells (10 μl) were prepared by placing acetone-washed, 18 $\times$ 18 mm glass coverslips over two parallel strips of double-sided tape on a glass slide. Sea urchin sperm axonemes in 5 mM imidazole/NaOH (pH 7), 100 mM NaCl, 4 mM $MgSO_4$, 1 mM $CaCl_2$, 0.1 mM EDTA, 0.1 mM ATP, 7 mM β-mercaptoethanol, and 50% glycerol were diluted 1:200 in 1 $\times$ BRB80, introduced into the flow cell, and incubated at room temperature for 4 min to allow axonemes to adhere to the glass surface. Next, approximately 1.5 mg/ml bovine brain tubulin in 10% DMSO, 1 mM GTP, and 0.5$\times$ BRB80 was introduced into the flow cell and the flow cell was placed on a 37°C heat block for 10 min to allow microtubules to polymerize off the ends of the axonemes. The tubulin concentration was titrated to generate axoneme–microtubule structures with much longer microtubules on one end than the other, and few microtubules free in solution. After the 10-min incubation, BRB80 containing 20 μM taxol at 37°C was introduced to stabilize the polymerized microtubules. Flow cells were stored for up to 2 days in a hydrated chamber.

Organelle transport assays. The flow cell was first washed with 10 μl of LB/15% sucrose to remove any free microtubules, followed by the introduction of 10 μl of assay mix consisting of, in the case of extracts, 2 μl PNS,

7.5 µl LB/15% sucrose, and 0.5 µl of a 20× ATP regenerating mix (20 mM ATP, 20 mM $MgCl_2$, 40 mM creatine phosphate, and 40 U/ml creatine kinase). For assessing motility in the presence of vanadate, aliquots of freshly made PNS were incubated with 2 mM ATP, 5 mM $MgCl_2$, 4 mM creatine phosphate, 4 U/ml creatine kinase, 2 mM DTT, and 40 µM sodium orthovanadate for at least 10 min on ice prior to beginning motility assays. Assay mixes for the HSS and ATP releasate fractions consisted of 5 µl HSS/ATP releasate, 3.5 µl LB/15% sucrose, 1 µl KI-washed vesicles (see above), and 0.5 µl ATP-regenerating mix. Assay mixes for more highly purified fractions such as the ''salt wash'' or post-salt wash ATP releasate consisted of 4 µl of the fraction, 4 µl LB/15% sucrose, 1 µl KI-washed vesicles, 0.5 µl of a 20-mg/ml casein stock, and 0.5 µl ATP-regenerating mix. If extracts with fluorescently labeled vesicles were to be observed, 0.5 µl of a 20× oxygen scavenger mix was added to the assay mix, maintaining a total final volume of 10 µl (20× oxygen scavenger mix: 20 mM DTT, 2 mg/ml glucose oxidase, 0.36 mg/ml catalase, and 0.24 M glucose; all stocks made separately in BRB80 and combined just before use). The movement of organelles in unlabeled extracts was observed using a Zeiss Axioplan microscope equipped with differential interference contrast (DIC) optics, a 50- or 100-W mercury arc lamp, and a 100×, 1.3 NA Plan-Neofluor objective. Images were detected using a camera (Newvicon; Hamamatsu Photonics, Bridgewater, NJ); contrast enhancement and background subtraction were performed with an image processor (Argus10; Hamamatsu Photonics), and recordings were made with a super VHS video tape recorder (AG-5700; Panasonic, Secaucus, NJ). Single-frame images were captured from video tape onto a Macintosh 8100/100, using VideoVision Frame Grabber and Photoshop software. To observe the movement of rhodamine-labeled organelles, the axoneme-nucleated microtubule array was first visualized by DIC as described above. The same field was then viewed using a 100-W tungsten lamp and a SIT camera (to confirm the location of the unlabeled axoneme), followed by observation of the fluorescent vesicles moving in the same field by fluorescence optics using the SIT camera.

Organelle motility was quantified by counting the number of vesicles moving per minute in each direction on a single axoneme/microtubule structure. Only axonemes with clearly defined polarity were used. Recordings of movement were performed on axonemes with between 6 and 12 microtubules (8–14 µm each in length) polymerized from the plus ends. If an organelle paused briefly and then continued in the same direction, it was scored as a single movement. Velocities of movements were quantified using custom software; only vesicles which moved smoothly over a distance of at least 1.5–2 µm were scored.

Dynein Membrane Association and Protein Analysis

PNS (320 µl prepared as described above) was made to 1.5 M sucrose by adding LB/2 M sucrose (680 µl) and layered above a 400-µl cushion of LB/2 M sucrose and below 400-µl and 500-µl layers of LB/1.4 M sucrose and LB/0.25 M sucrose, respectively. The membranes were then isolated by flotation to the 1.4 M/0.25 M sucrose interface by centrifugation at 200,000*g* for 30 min in a Beckman TLS 55 rotor (4°C). To assess the affinity of motor binding to the membranes, one-half of the floated membranes were diluted 1:5 in LB and repelleted by centrifugation at 175,000*g* for 15 min in a Beckman TLA 120.1 rotor (4°C).

Samples were separated on 4–12% or 5–15% gradient polyacrylamide gels under denaturing and reducing conditions. Gels were either stained with colloidal Coomassie or electroblotted to nitrocellulose membranes at 100 mA for 75 min. The blots were incubated with either a polyclonal antibody against the conserved kinesin LNLVDLAGSE domain (1 µg/ml) [Sawin et al., 1992] or an affinity-purified polyclonal antibody against the *Dictyostelium* dynein heavy chain (1:1,000) [Koonce and Samso, 1996] overnight at 4°C, and then incubated in HRP-conjugated secondary antibody (1:2,000; Amersham Life Sciences, Arlington Heights, IL) for 1 hr at room temperature. Blots were developed using a chemiluminescence kit (NEN Life Sciences, Beverly, MA) and exposed to Hyperfilm (Amersham).

RESULTS

An In Vitro Assay for Microtubule-Based Movements in *Dictyostelium* Cell Extracts

By refining buffer and protease inhibitor conditions, we developed a method for preparing *Dictyostelium* extracts that displayed robust bidirectional microtubule-based vesicle transport. The crude extract supported more than 30 vesicle movements/min per axoneme structure (Table I); this activity lasted for hours on ice and was stable to freeze-thaw in liquid nitrogen. The presence of fresh PMSF in the extract was found to be particularly important for maintaining the transport activity. In order to assess the directionality of movement of the *Dictyostelium* vesicles, a polarized array of microtubules was assembled by polymerizing bovine brain tubulin from the ends of sea urchin axonemes. The plus ends of microtubules could be identified by the significantly longer microtubules that grew off of one end of the axoneme [Allen and Borisy, 1974]. Vesicles moved bidirectionally on microtubules, with vesicles moving smoothly from axoneme to microtubule and vice-versa. Individual vesicles were often observed to change direction one or more times, and frequently paused midway through the

TABLE I. Frequencies and Velocities of Vesicle Movements in Wild-Type *Dictyostelium* Extracts*

	Frequency (movt/min/axoneme)		Velocity (μm/s)	
	Minus end	Plus end	Minus end	Plus end
A. PNS	26.7 ± 2.1	6.2 ± 0.7	2.74 ± 0.40	2.04 ± 0.30
B. HSS	15.3 ± 0.7	3.6 ± 1.1	2.75 ± 0.42	2.13 ± 0.38
C. ATP releasate	17.0 ± 2.8	5.9 ± 3.6	2.77 ± 0.49	2.11 ± 0.33

*Frequency of vesicle movements was quantified as movements per minute in each direction over a period of 4 min on microtubules nucleated off of a single axoneme (see under Materials and Methods). Frequencies represent the mean ± SD for the averages from n = 3, n = 2, and n = 3, separate preparations of PNS, HSS, and ATP releasate, respectively. For each preparation, one to four separate assays were performed and the results averaged. The velocities represent the mean ± SD for a total of n = 149, n = 35, and n = 93 minus end movements and n = 82, n = 16, and n = 51 plus end movements measured over all of the preparations of PNS, HSS, and ATP releasate, respectively.

length of their movement. Minus end-directed motility was approximately four times more frequent than plus end-directed motility, and the speeds of movement in the minus end direction were faster than in the plus end direction (Table I).

As *Dictyostelium* has been widely used as a model system for the study of endocytosis [e.g., Bacon et al., 1994; Bush et al., 1996; Padh et al., 1993], we also adapted our *Dictyostelium* assay to observe specifically the motility of endocytic vesicles in vitro. To achieve this, cells were incubated with rhodamine-conjugated dextran, a marker which is internalized by fluid-phase endocytosis. Wild-type cells incubated for 20 min with rhodamine-dextran at room temperature showed bright vesicular labeling when viewed by fluorescence microscopy, while cells that had been subjected to the same pulse at 4°C to inhibit endocytosis showed no labeling (data not shown). When extracts were prepared, fluorescent vesicles were observed moving along microtubules (Fig. 1). Most of the fluorescent vesicle movements were to the minus end of the microtubules/axoneme, although the ratios of minus to plus end-directed movements varied from preparation to preparation for reasons that are still unclear. The velocities of the endocytic vesicle movements were similar to those of the unlabeled vesicle population observed by DIC microscopy (minus end-directed: 2.2 ± 0.4 μm/sec, n = 58; plus end-directed: 1.8 ± 0.3 μm/sec, n = 27). Many of the labeled vesicles moved bidirectionally: over 80% (n = 49) of the endocytic vesicles that moved toward the plus end also exhibited at least one episode of minus end-directed movement. In contrast, only 60% (n = 76) of the total vesicle population (endocytic as well as others) in a typical crude extract observed by DIC microscopy exhibited such behavior.

The high level of minus end transport in the extracts suggests that cytoplasmic dynein may be the predominant motor functioning in this system. Dynein-generated motility has been shown to be more sensitive to inhibition by sodium orthovanadate than kinesin motility [Shimizu, 1995]; we therefore tested the effect of sodium orthovanadate on activity in the extracts. The addition of 40 μM vanadate to the PNS inhibited minus end-directed transport by approximately fourfold, reducing the number of minus end movements per minute per axoneme from 16.5 ± 4.7 to 4.1 ± 1.2 (n = 6 assays over two separate extracts). However, 40 μM vanadate did not inhibit the plus end-directed movements (2.4 ± 0.9 and 1.8 ± 0.3 movements/min/axoneme in the presence and absence of vanadate, respectively). These results are consistent with the involvement of cytoplasmic dynein in minus end-directed motility in this system.

Requirements for Vesicle Transport

To better define the protein requirements of the *Dictyostelium* vesicle transport assay, we examined whether soluble factors are necessary or whether all the factors required for transport are tightly bound to membranes as has been described in other studies [Muresan et al., 1996; Schnapp et al., 1992]. When vesicles were separated from soluble cytosolic components in the PNS by centrifugation through a sucrose cushion, the isolated vesicles exhibited full levels of motility in the plus end direction but no movement in the minus end direction (data not shown). When the vesicle pellet was washed in either buffer alone or buffer plus 0.3 M KI and then repelleted and resuspended, the vesicles did not move in the absence of cytosol. However, recombination of these ''washed'' vesicles with the HSS generated robust motility similar to that in the PNS (Table I). Therefore, the components necessary for plus end transport appear to be initially bound, albeit weakly, to the vesicle surface; in contrast, minus end motility is lost during vesicle isolation and requires the addition of soluble factors.

We next examined whether cytosolic factors that stimulate the transport of 0.3 M KI-washed organelles could be partially purified from the HSS by enriching for microtubule motor proteins, as has been successfully utilized in other reports [Schroer and Sheetz, 1991]. A microtubule motor-containing fraction was prepared by incubating the HSS with taxol-stabilized microtubules in the presence of hexokinase, glucose and AMP-PNP to cause tight binding of motors to microtubules, collecting the microtubules by centrifugation, and releasing motors from microtubules by the addition of 5 mM Mg^{2+}ATP. This ''ATP releasate,'' in combination with 0.3 M KI-washed vesicles, supported robust bidirectional vesicle transport at levels similar to those in the PNS and HSS

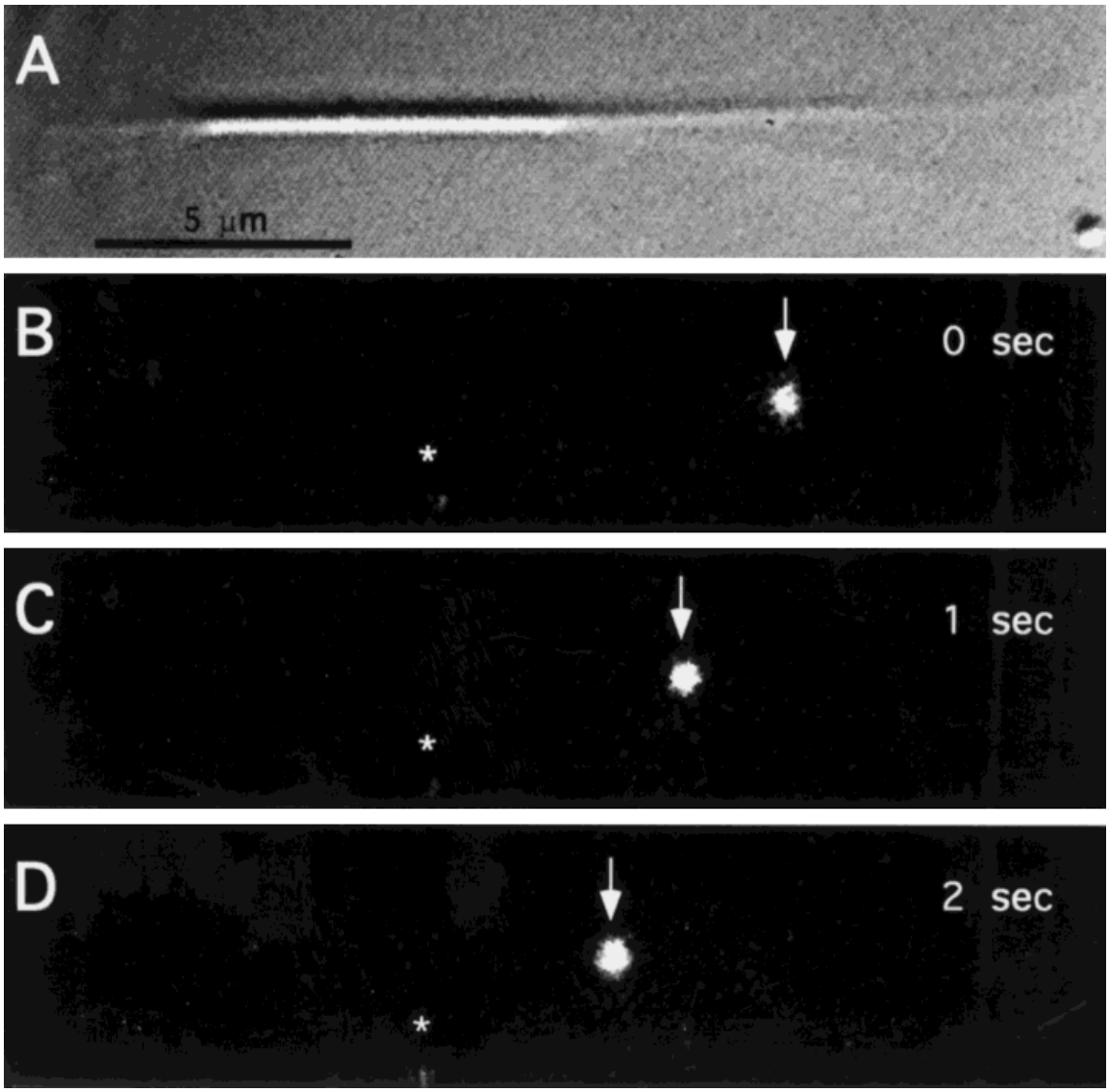

Fig. 1. Endocytic vescicles from *Dictyostelium* extracts move along microtubules in vitro. Endocytic vesicles were fluorescently labeled by incubating cells with rhodamine-conjugated dextran for 20 min to allow fluid-phase uptake of the marker, followed by preparation of extracts (see under Materials and Methods). **A:** DIC microscopic image of a sea urchin axoneme with nucleated bovine brain microtubules which was the substrate for the assay. The plus end is identified by the longer microtubules emerging from one end of the axoneme. **B–D:** Movement of an endocytic vesicle (*arrow*) in the same assay field visualized by fluorescence microscopy. This vesicle is moving toward the minus end of the microtubule. The star (★) indicates a stationary fluorescent vesicle, for comparison. Bar = 5 μm.

(Table I). The velocities of the moving vesicles were equivalent in the PNS, HSS, and ATP releasate (Table I).

We then tested whether the plus end- and minus end-directed transport activities could be separated from each other on the basis of differences in their microtubule affinities. We found that washing the microtubule pellet with buffer containing 0.3 M KCl before incubating the microtubules with Mg/ATP generated a ''salt wash'' fraction with predominantly minus end activity and very little plus end activity. A subsequent incubation of the salt-washed microtubules with Mg/ATP resulted in an ATP releasate that was significantly depleted of minus end activity, but that contained abundant plus end activity (Fig. 2A). Combination of the salt wash and ATP releasate fractions did not produce levels of activity that were higher than the sum of the individual activities (data not shown). The two fractions were subjected to electrophoresis (Fig. 2B) and immunoblotting with antibodies against the dynein heavy chain and against a conserved sequence in the kinesin motor domain (LNLVDLAGSE) (Fig. 2C). The DHC is enriched in the salt-wash fraction relative to the ATP releasate, and the relative amounts in

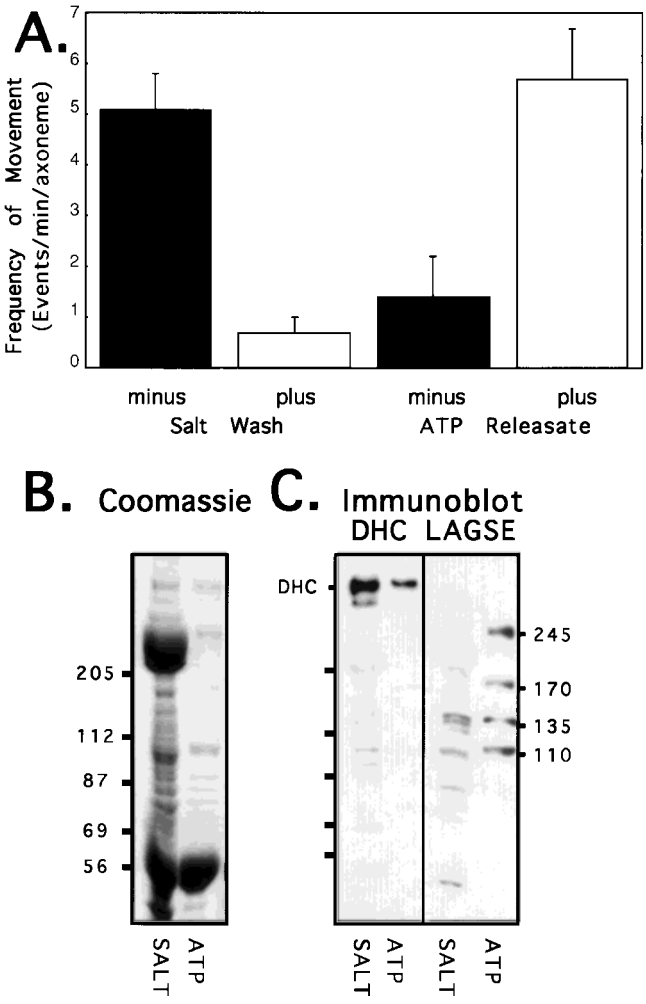

Fig. 2. Separation of minus end- and plus end-directed transport activities by differential microtubule affinity. High-speed supernatant (HSS) was incubated with microtubules, taxol, ATP-depleting reagents, and AMP-PNP. Microtubules were collected by centrifugation, resuspended in buffer containing 0.3 M KCl, and then re-sedimented. The supernatant (''salt wash'') was dialyzed into assay buffer, while the pellet was further eluted with buffer containing Mg^{2+} ATP (see under Materials and Methods). **A:** Frequencies of plus end- and minus end-directed vesicle movements in the salt wash and the ATP releasate. Most of the plus end activity is retained in the ATP releasate, while the salt wash contains predominantly minus end activity. Frequencies were quantified as described in the legend to Table I. Values are averaged over three 4-min assays performed on each of three separate preparations of the two fractions. Error bars represent standard error of the mean (SEM) of the individual averages of the three preparations. **B:** Coomassie-stained gel (sodium dodecyl sulfate-polyacrylamide gel electrophoresis [SDS-PAGE]) demonstrating the protein composition of the salt wash and ATP releasate. The positions of molecular weight standards are indicated on the left side of B. The thick band of approximately 245-kDa present in the salt wash is myosin, as evidenced by immunoblots using antibodies against *Dictyostelium* myosin II (not shown). **C:** Immunoblots of the two fractions using an antibody against the *Dictyostelium* dynein heavy chain and a pan-kinesin antibody (anti-LAGSE). *Tick marks* (*left*), indicate the positions of the same five molecular weight standards labeled in B. The DHC is more prominent in the salt wash fraction, whereas four LAGSE-positive bands are enriched in the ATP releasate.

these two fractions correlate reasonably well with the distribution of minus end transport activity. These results further support the idea that cytoplasmic dynein is a minus end-directed organelle transport motor in this system. Conversely, four LAGSE-reactive polypeptides of approximately 245, 170, 135, and 110 kDa are selectively present in the ATP releasate compared to the salt wash, representing potential candidates for kinesin motors that may power plus end transport activity in the ATP releasate.

Overexpression of the Globular Head of Cytoplasmic Dynein Disrupts Minus End-Directed Transport

A *Dictyostelium* cell line overexpressing a C-terminal 380-kDa fragment (amino acids [aa] 1384–4725; Fig. 3A) comprising the globular head of cytoplasmic dynein (380-kDa cells; [Koonce and Samso, 1996]) displays an intriguing phenotype in which the interphase radial microtubule network can be collapsed in a whorl around the nucleus. It was suggested that this phenotype could be due to the overexpressed fragment interfering with an interaction of wild-type dynein with membranes or microtubules at the microtubule–plasma membrane interface [Koonce and Samso, 1996]. To test the possibility that the observed phenotype could be somehow correlated with a defect in dynein association with membranes and/or membrane transport, we examined vesicle motility in the 380-kDa cells using our in vitro assay. As shown in Figure 3B and C, the frequency of minus end-directed organelle movements was reduced in 380-kDa cells by 41% ($P < 0.002$) relative to the wild-type cells, while the frequency of plus end-directed movements was equivalent in the two cell types. Similarly, the velocity of minus end movements was reduced by 20% ($P < 0.001$) in the 380-kDa cell, relative to wild type, while the velocities of plus end-directed movements were equivalent.

The fact that the plus end-directed movements were unaffected in the 380-kDa cells shows that the observed defects in minus end transport are specific and are not likely to be attributable to a generalized defect in metabolic or cellular function. To further confirm this point, we also examined cells overexpressing a 318-kDa fragment of the DHC (deletion of a.a. 3105–3643 from the 380-kDa polypeptide) in our assay. The deletion in this construct is within the globular head domain, and it is unclear if this construct is folded in the same manner as the wild-type head domain; however, the 318-kDa fragment is expressed at the same levels as the 380-kDa fragment and is soluble. In contrast to the 380-kDa cells, we saw no defect in minus end transport in the 318-kDa cells relative to wild-type cells assayed in parallel (data not shown). Thus, protein overexpression alone is not

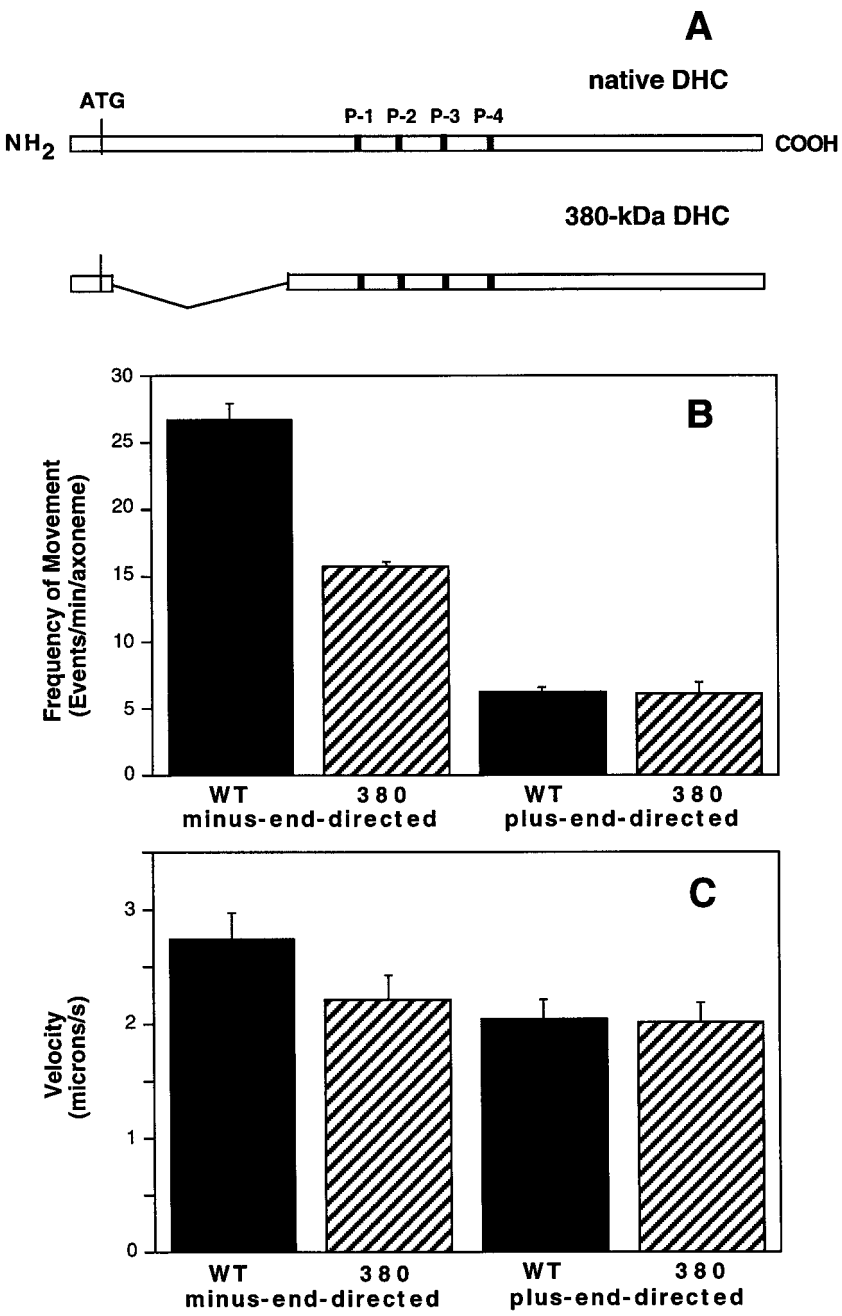

Fig. 3. The frequency and velocity of minus end-directed transport are reduced in extracts from the 380-kDa cells. **A:** The 380-kDa DHC construct as compared with the full-length DHC. The 380-kDa construct encodes the first 12 amino acids at the N-terminus, a linker encoding 3 a.a., and a.a. 1384–a.a. 4725. Closed boxes labeled P-1 through P-4 indicate P-loop motifs that form part of consensus sequences for ATP-binding domains. **B,C:** Frequencies (**B**) and velocities (**C**) of vesicle movements were quantified as described in the legend to Table I. Values are averaged over three 4-minute assays performed on each of three separate preparations of PNS from wild-type or 380-kDa cells. Error bars represent standard error of the mean (SEM) of the individual averages of the three preparations. *t*-test statistical analysis showed a statistically significant difference between the frequency and velocity of minus end-directed movements in WT vs. 380-kDa cells ($P < 0.002$), while the frequency and velocity of plus end-directed movements were equivalent within statistical limits in the two cell types. Total numbers of movements scored for velocity measurements were n = 149 and n = 133 minus end movements and n = 82 and n = 83 plus end movements for WT and 380-kDa cells, respectively.

responsible for the defect observed in minus end transport in the 380-kDa cells.

The 380-kDa Head Fragment Binds to Membranes In Vitro

The in vitro motility data suggests that the globular head is in some way able to interfere with minus end-directed vesicle transport. To examine whether this effect may be due to a dominant negative interaction that involves binding of the 380-kDa fragment to membranes, membranes from the PNS were isolated by flotation on a discontinuous sucrose gradient and the amount of DHC present was analyzed by immunoblotting. The 380-kDa fragment was associated with membranes prepared from the 380-kDa cells (Fig. 4B). However, the amount of full-length DHC bound to those membranes was similar to that in wild-type cells, suggesting that the fragment does not compete with full-length DHC for binding in vivo. When the membranes were diluted in buffer and then reisolated by sedimentation, the majority of the membrane-bound 380-kDa fragment dissociated while the full-length heavy chain was retained on the mem-

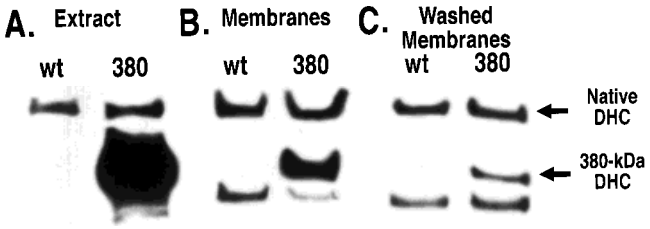

Fig. 4. Binding of the 380-kDa fragment to membranes. Membranes from extracts of wild-type (WT) and 380-kDa cells were isolated by flotation on a discontinuous sucrose gradient (see under Materials and Methods). **A:** Immunoblot of postnuclear supernatant (PNS) before centrifugation. *Arrows* (*right*), indicate the location of the native DHC and the 380-kDa DHC fragment. **B:** Immunoblot of membranes collected from the 1.4 M/0.25 M sucrose interface after centrifugation. The 380-kDa fragment binds to membranes but does not reduce the amount of bound full-length DHC. The band below 380-kDa that appears in both cell types may be a degradation product recognized by the DHC antibody, as it increases with time of sample storage. **C:** Membranes isolated as in B, which were diluted 1:5 in lysis buffer and then collected by centrifugation. Comparison of B and C shows that most of the 380-kDa fragment dissociated from the membranes, whereas the full-length DHC remained bound.

branes (Fig. 4C). Thus, although the 380-kDa fragment can bind to membranes, its affinity is lower than that of the native DHC.

DISCUSSION

In this study, we have developed an in vitro assay for microtubule-based organelle transport in *Dictyostelium*, an organism tractable by both biochemical and molecular genetic approaches. Early studies reported occasional microtubule-based movements of vesicles in *Dictyostelium* extracts [McCaffrey and Vale, 1989], but such results were not consistently observed. By using an appropriate combination of buffer, protease inhibitor, and cell breakage conditions, we now can obtain robust movement in a reproducible manner. Vesicle transport can be reconstituted by recombining a high speed supernatant or a microtubule affinity-purified motor fraction with KI-washed organelles. We have also been able to separate the minus end and plus end transport activities by exploiting a difference in the salt sensitivity of their interactions with microtubules. The minus end activity can be eluted from microtubules by a wash in buffer containing 0.3 M KCl, while most of the plus end activity is retained on the microtubules during the wash and is only eluted by buffer containing 5 mM Mg/ATP. Immunoblots of the two fractions show that the DHC is more abundant in the salt wash than in the ATP releasate, correlating well with the distribution of minus end activity. The immunoblots further reveal four candidate kinesin motors in the ATP releaseate that may be involved in supporting some or all of the plus end-directed vesicle movements. This two-step elution protocol, which removes much of the dynein and myosin as well as many other polypeptides in the salt wash, provides a good starting point for further purification of the plus end transport activity.

Identifying all the components needed for organelle transport and defining their functions represent important goals for the organelle transport field. Whether components required for motility are tethered to membranes or are predominantly soluble remains controversial. In the *Dictyostelium* extracts, we have shown that the plus end transport activity is retained on vesicles upon initial isolation, though it can be subsequently removed by either a buffer or 0.3 M KI wash. By contrast, movement of vesicles in the minus end direction is dependent entirely on the addition of cytosol. This difference in the requirements for soluble factors for minus and plus end-directed vesicle transport has also been documented in squid axoplasm [Muresan et al., 1996; Schnapp et al., 1992]. However, in the squid system, components required for plus end transport remain tightly bound to vesicles even after stringent washes. It is unclear whether our results and those of other groups reflect a difference in the relative affinities of the plus end and minus end motors for membranes or, alternatively, a difference in the requirements for soluble accessory factors to activate membrane-bound motors, (e.g. dynactin for dynein-based motility; [Blocker et al., 1997; Gill et al., 1991; Schroer and Sheetz, 1991]). The assay system described here potentially can be exploited to address these issues by defining the complete set of factors necessary for the transport of an organelle.

Another approach to investigating the molecular mechanisms of organelle transport is to create mutants in known motor proteins or other factors and to examine both the in vivo and in vitro effects of the mutations on transport. While such studies are underway in *Drosophila* [Saxton et al., 1991] and have produced interesting in vivo phenotypes, in vitro organelle transport assays have not yet been developed for *Drosophila*. In *Dictyostelium*, a cell line overexpressing the globular head domain of cytoplasmic dynein was recently created (380-kDa cells; [Koonce and Samso, 1996]), representing the first available *Dictyostelium* mutant in a microtubule-based motor protein. These cells displayed a striking phenotype in which the normally radial array of interphase microtubules was collapsed toward the cell center. To examine whether this in vivo phenotype might be associated with a defect in membrane transport, we analyzed organelle transport in the 380-kDa cells using our in vitro assay. We have shown that the frequency and velocity of minus end transport were reduced in the 380-kDa cells by 40% and 20%, respectively, relative to wild-type cells. In contrast, the frequency and velocity of plus end-directed movements were equivalent in the two cell types. We have also

attempted to compare in vivo vesicle movements in the wild-type and 380-kDa cells, but these efforts were complicated by the difficulty in establishing the polarity of the in vivo movements, particularly in the 380-kDa cells which have a collapsed microtubule network.

Our in vitro organelle transport results are consistent with the suggestion by Koonce and Samso [1996] that the phenotype of the 380-kDa cells could represent a defect in dynein–membrane–microtubule interactions. The collapse of the microtubule network in the 380-kDa cells would seem to imply a specific defect in dynein-based interactions between the plasma membrane and the microtubule network that would normally serve to maintain the radial array of microtubules. Although we did not investigate the motility of plasma membrane vesicles specifically, the results of our examination of total vesicle motility are generally consistent with such a hypothesis.

Given our observation of a specific defect in minus end transport in the 380-kDa cells, what could be the molecular basis for such a defect? At the present time, the answer is unclear. One possibility is that the 380-kDa fragment could physically interfere with minus end transport by binding to microtubules and sterically blocking transport. However, such binding would most likely disrupt both plus end- and minus end-directed transport, which was not observed. Additionally, the 380-kDa fragment does not colocalize with microtubules by immunofluorescence in overexpressing cells [Koonce and Samso, 1996]. A second possibility is that the 380-kDa fragment could somehow be interfering with minus end transport by binding to membranes and exerting a dominant negative effect. In support of this idea, we have shown that the 380-kDa fragment is associated with endogenous membranes. However, its affinity for membranes is weaker than that of native dynein and it does not appear to compete with the native DHC for binding. Potentially, the membrane-bound 380-kDa fragment could exert a dominant negative effect if it interacts abnormally with microtubules and/or prevents native dynein interaction and motility. Although the precise mechanism cannot be further elucidated from the present data, the decrease in both frequency and velocity of organelle movement is consistent with this general hypothesis. An alternative possibility for a potential dominant negative action is that the 380-kDa fragment could titrate out a factor important for dynein function. One candidate for such an interaction is the 58-kDa dynein subunit, which has been shown to partially comigrate with the 380-kDa fragment upon centrifugation on a sucrose gradient [Koonce and Samso, 1996]. Alternatively, there may be small accessory light chains associated with *Dictyostelium* cytoplasmic dynein similar to those associated with mammalian brain dynein [King et al., 1996], any of which could potentially be titrated by the 380-kDa fragment.

Overall, the use of *Dictyostelium* for in vitro studies of organelle transport offers several advantages. First, our assay displays an extremely robust level of activity, supporting more movement than *Xenopus* egg extracts [e.g., Niclas et al., 1996] or mammalian extracts [e.g., Blocker et al., 1997; Schroer and Sheetz, 1991]. Second, it is possible to generate far larger quantities of material for biochemical experiments than can be obtained in other systems that display highly active organelle transport in vitro, such as squid axoplasm. Thus, the assay described here can be used to purify motors that stimulate organelle transport, as well as to identify accessory factors that may work in concert with these motors [Blocker et al., 1997; Gill et al., 1991; Schroer and Sheetz, 1991]. Finally, the effects of additional mutations in microtubule-based motors or accessory factors can be examined using this assay system.

ACKNOWLEDGMENTS

We thank members of the Vale laboratory for their helpful discussions. N.P. is a student in the Medical Scientist Training Program. M.K. is supported by NIH grant GM51532. E.L.de H. is supported by a Career Development Award from the American Heart Association. R.D.V. is supported in part by NIH grant 38499.

REFERENCES

Allan, V. (1995): Membrane traffic motors. FEBS Lett. 369:101–106.

Allen, C., and Borisy, G.G. (1974): Structural polarity and directional growth of microtubules of flagella. J. Mol. Biol. 90:381–402.

Bacon, R.A., Cohen, C.J., Lewin, D.A., and Mellman, I. (1994): *Dictyostelium discoideum* mutants with temperature-sensitive defects in endocytosis. J. Cell Biol. 127:387–399.

Blocker, A., Severin, F.F., Burkhardt, J.K., Bingham, J.B., Yu, H., Olivo, J.C., Schroer, T.A., Hyman, A.A., and Griffiths, G. (1997): Molecular requirements for bi-directional movement of phagosomes along microtubules. J. Cell Biol. 137:113–129.

Bush, J., Temesvari, L., Rodriguez-Paris, J., Buczynski, G., and Cardelli, J. (1996): A role for a rab4-like GTPase in endocytosis and in regulation of contractile vacuole structure and function in *Dictyostelium discoideum*. Mol. Biol. Cell 7:1623–1638.

De Lozanne, A., and Spudich, J.A. (1987): Disruption of the *Dictyostelium* myosin heavy chain gene by homologous recombination. Science 236:1086–1091.

Gill, S.R., Schroer, T.A., Szilak, I., Steuer, E.R., Sheetz, M.P., and Cleveland, D.W. (1991): Dynactin, a conserved, ubiquitously expressed component of an activator of vesicle motility mediated by cytoplasmic dynein. J. Cell Biol. 115:1639–1650.

Goodson, H.V., Valetti, C., and Kreis, T.E. (1997): Motors and membrane traffic. Curr. Opin. Cell Biol. 9:18–28.

Hill, K.L., Catlett, N.L., and Weisman, L.S. (1996): Actin and myosin function in directed vacuole movement during cell division in *Saccharomyces cerevisiae*. J. Cell Biol. 135:1535–1549.

Huffaker, T.C., Thomas, J.H., and Botstein, D. (1988): Diverse effects of B-tubulin mutations on microtubule formation and function. J. Cell Biol. 106:1997–2010.

Jung, G., and Hammer, J.A. III (1990): Generation and characterization of *Dictyostelium* cells deficient in a Myosin I heavy chain isoform. J. Cell Biol. 110:1955–1964.

King, S.M., Barbarese, E., Dillman, J.F.I., Patel-King, R.S., Carson, J.H., and Pfister, K.K. (1996): Brain cytoplasmic and flagellar outer arm dyneins share a highly conserved M_r 8,000 light chain. J. Biol. Chem. 271:19358–19366.

Konnce, M.P. and Knecht, D.A. (1998): The cytoplasmic dynein heavy chain is an essential gene product in *Dictyostelium*. Cell Motil. Cytoskeleton 39:63-72.

Koonce, M.P., and McIntosh, J.R. (1990): Identification and immunolocalization of cytoplasmic dynein in *Dictyostelium*. Cell Motil. Cytoskeleton 15:51–62.

Koonce, M.P., and Samso, M. (1996): Overexpression of cytoplasmic dynein's globular head causes a collapse of the interphase microtubule network in *Dictyostelium*. Mol. Biol. Cell 7:935–948.

Koonce, M.P., Grissom, P.M., Lyon, M., Pope, T., and McIntosh, J.R. (1994): Molecular characterization of a cytoplasmic dynein from *Dictyostelium*. J. Eukaryote Microbiol. 41:645–651.

Kuspa, A., and Loomis, W.F. (1994): Transformation of *Dictyostelium*: Gene disruptions, insertional mutagenesis, and promoter traps. Methods Mol. Genet 3:3–21.

Lenhard, J.M., Mayorga, L., and Stahl, P.D. (1992): Characterization of endosome–endosome fusion in a cell-free system using *Dictyostelium discoideum*. J. Biol. Chem. 267:1896–1903.

Malchow, D., Naegele, B., Schwarz, H., and Gerisch, G. (1972): Membrane-bound cyclic AMP phosphodiesterase in chemotactically responding cells of *Dictyostelium discoideum*. Eur. J. Biochem. 28:136–142.

McCaffrey, G., and Vale, R.D. (1989): Identification of a kinesin-like microtubule-based motor protein in *Dictyostelium discoideum*. EMBO J.8:3229–34.

Muresan, V., Godek, C.P., Reese, T.S., and Schnapp, B.J. (1996): Plus end motors override minus-end motors during transport of squid axon vesicles on microtubules. J. Cell Biol. 135:383–397.

Niclas, J., Allan, V.J., and Vale, R.D. (1996): Cell cycle regulation of dynein association with membranes modulates microtubule-based organelle transport. J. Cell Biol. 133:585–593.

Novick, P., and Botstein, D. (1985): Phenotypic analysis of temperature-sensitive yeast actin mutants. Cell 40:405–416.

Padh, H., Ha, J., Lavasa, M., and Steck, T.L. (1993): A post-lysosomal compartment in *Dictyostelium discoideum*. J. Biol. Chem. 268:6742–6747.

Roos, U.-P., De Brabander, M., and De Mey, J. (1984): Indirect immunofluorescence of microtubules in *Dictyostelium discoideum*. A study with polyclonal and monoclonal antibodies to tubulins. Exp. Cell Res. 151:183–193.

Roos, U.-P., De Brabander, M., and Nuydens, R. (1987): Movements of intracellular particles in undifferentiated amebae of *Dictyostelium discoideum*. Cell Motil. Cytoskel. 7:258–271.

Ruscetti, T., Cardelli, J.M, Niswonger, M L., and O'Halloran, T.J. (1994): Clathrin heavy chain functions in sorting and secretion of lysosomal enzymes in *Dictyostelium discoideum*. J. Cell Biol. 126:343–352.

Sawin, K.E., Mitchison, T.J., and Wordeman, L.G. (1992): Evidence for kinesin-related proteins in the mitotic apparatus using peptide antibodies. J. Cell Sci. 101:303–313.

Saxton, W.M., Hicks, J., Goldstein, L.S., and Raff, E.C. (1991): Kinesin heavy chain is essential for viability and neuromuscular functions in *Drosophila*, but mutants show no defects in mitosis. Cell 64:1093–1102.

Schnapp, B.J., Reese, T.S., and Bechtold, R. (1992): Kinesin is bound with high affinity to squid axon organelles that move to the plus-end of microtubules. J. Cell Biol. 119:389–399.

Schroer, T.A., and Sheetz, M.P. (1991): Two activators of microtubule-based vesicle transport. J. Cell Biol. 115:1309–1318.

Shimizu, T. (1995): Inhibitors of the dynein ATPase and ciliary or flagellar motility. Methods Cell Biol. 47:497–501.

Spudich, J.A. (1987): Introductory remarks and some biochemical considerations. Methods Cell Biol. 28:3–8.

Sussman, M. (1987): Cultivation and synchronous morphogenesis of *Dictyostelium* under controlled experimental conditions. Methods Cell Biol. 28:9–29.